Semana de la Nanociencia y la Nanotecnología en Colombia 2013 (SNNC 2013)

UNIVERSIDAD DE ANTIOQUIA
1803

CONTRIBUCIONES ACEPTADAS COMO PÓSTER PARA NANOANTIOQUIA'2013 (Jueves 18 de julio, Hall 1 piso EIA-Sede Zuñiga)	
Leonardo Rafael Medrano Sandonas	Influencia de parámetros de desorden sobre las propiedades estructurales y electrónicas de nano-partículas y nano-hilos de plata
Maria de Jesus de Matos Gomes	Microstructure and optical properties of ZnO nanocrystals embedded in Al2O3 matrix
Maria Fernanda Pilaquinga Flores	Análisis rápido de remoción de varias especies químicas en agua usando nanopartículas magnéticas de hierro
Marlon Rincón Fulla	Hydrostatic pressure and magnetic field effects on the D- ion energy structure in toroidal quantum ring
Marlon Rincón Fulla	Ión D- en anillos cuánticos concéntricos: Efecto de la presión hidrostática y del campo magnético
Marlon Rincón Fulla	Niveles energéticos bi-electrónicos en nano-anillos apilados: Influencia de la presión hidrostática
Marlon Rincón Fulla	Two-particle systems in quantum ribbons and rings: The effects of dimensionality and external fields
Marta Ramos	Optical emission spectroscopy study of pulsed laser deposition of semiconducting nanoparticles
Miguel Eduardo Mora Ramos	Topología de vórtices en condensados de Bose-Einstein de polaritones excitónicos en microcavidades
Paulo Noronha Lisboa-Filho	Sonochemical Effects in ZnO Particles
Paulo Noronha Lisboa-Filho	One-dimensional TiO2 Nanostructures and their Morphological and Optical Properties
Ricardo León Restrepo Arango	Propiedades ópticas no lineales en anillos cuánticos semiconductores
Rolando Pérez Álvarez	Coeficiente de Transmisión y Escape de Barreras Gaussianas y Regulares
Santiago Pèrez Walton	Propiedades estructurales, electrónicas y ópticas de las fases α y β del cuarzo
Willian Gutiérrez Niño	Charge distribution in type II Quantum Ring with captured exciton under magnetic field
Willian Gutiérrez Niño	Aharonov-Bohm oscillations in non-uniform nanoring under a lateral electric field
Yenisleidy de las Mercedes Zulueta Díaz	Nanotecnología en la purificación de aguas
Yurany Andrea González Jurado	Los nanomateriales: una alternativa para la obtención de biocombustibles a partir de celulosa
Zulamita Zapata Benabithe	Caracterización electroquímica de aerogeles de carbono dopados con nanopartículas metálicas para electrodos de supercondensadores

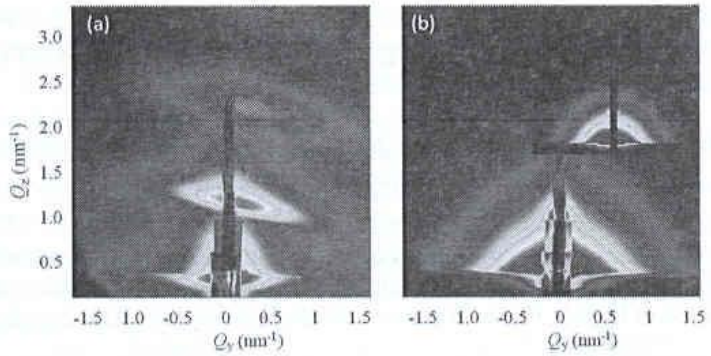

Fig. Typical 2D GISAXS intensity maps of (a) as-grown and (b) annealed ZnO/ Al2O3 multilayered nanostructure. The inset shows simulated GISAXS map

Keywords: Embedded ZnO nanocrystals, GISAXS, GIXRD, Photoluminescence

OPTICAL EMISSION SPECTROSCOPY STUDY OF PULSED LASER DEPOSITION OF SEMICONDUCTING NANOPARTICLES

L. Marques, M. M. D. Ramos*, M. J. M. Gomes

Centro de Física da Universidade do Minho, Campus de Gualtar, 4710-057 Braga, Portugal

* Autor a contactar: marta@fisica.uminho.pt.

Abstract

Memory devices that use seminconductor nanocrystals (NC) for charge storage began to receive considerable attention in recent years due to their excellent performance, high capacity of memory and miniaturization. In order to integrate these materials into devices, formation of NCs and oxide layers with controlled stoichiometry, dimensions and homogeneity are required. The optimization of nanoparticle synthesis by laser ablation requires the knowledge of the temporal and spatial scales for nanoparticle formation, and how the nanoparticles are transported and deposited. In this context, plasma optical emission spectroscopy (OES) is a convenient technique to monitor *in situ* and in real time the evolution of the induced plasma plume composition and species

kinetics. In this work, OES is used to determine the composition and energy of the plasma plume species obtained during ablation of seminconductor targets using a KrF excimer ns-laser (=248 nm). We have characterized the plasma plumes in vacuum, and in the presence of an argon atmosphere at 0.5 and 1 mbar. From registered emission spectra we obtained the electron temperature and density for different distances to the target, and laser fluences. The spatial dependence shows a decrease in electron temperature and density with distance.

Acknowlegments: This work was supported by the project (PTDC/FIS/098943/2008) funded by the Portuguese Foundation for Science and Technology (FCT).

Keywords: Nanoparticle, Optical emission Spectroscopy, Plume, Laser Ablation

Optical emission spectroscopy study of pulsed laser deposition of semiconducting nanoparticles.

L. Marques, M. M. D. Ramos*, M. J.M. Gomes

Centro de Física da Universidade do Minho, Campus de Gualtar, 4710-057 Braga, Portugal

Corresponding author: marta@fisica.uminho.pt

1.Introduction

Memory devices that use seminconductor nanocrystals (NC) for charge storage began to receive considerable attention in recent years due to their excellent performance, high capacity of memory and miniaturization. In order to integrate these materials into devices, formation of NCs and oxide layers with controlled stoichiometry, dimensions and homogeneity are required. The optimization of nanoparticle synthesis by laser ablation requires the knowledge of the temporal and spatial scales for nanoparticle formation, and how the nanoparticles are transported and deposited. In this context, plasma optical emission spectroscopy (OES) is a convenient technique to monitor *in situ* and in real time the evolution of the induced plasma plume composition and species kinetics. In this work, OES is used to determine the composition and energy of the plasma plume species obtained during ablation of seminconductor targets using a KrF excimer ns-laser (=248 nm) . We have characterized the plasma plumes in vacuum, and in the presence of an argon atmosphere at 0.5 and 1 mbar. From registered emission spectra we obtained the electron temperature and density for different distances to the target, and laser fluences. The spatial dependence shows a decrease in electron temperature and density with distance.

2. Experimental details

Pulsed Laser Deposition system

▪ **Laser type**	**Excimer KrF**
▪ **Laser wavelength**	**248 nm**
▪ **Laser energy**	**400 – 600 mJ**
▪ **Pulse duration**	**7 ns**
▪ **Target/substrate dist.**	**6 cm**
▪ **Targets**	**Si/Ge**
▪ **Pressure**	**10^{-6} – 1 mbar**
▪**Atmosphere**	**Argon**

Spectroscopy equipment

▪ ***Spectrometer***	***Ocean Optics HR 4000***
▪ ***Grating***	***HC-1 (300g/mm)***
▪ ***Resolution***	***0.5 nm***
▪***Optical fiber***	***Uv-Vis (Φ=1 mm)***

3. Computational details

First principles calculations of Si_2, Ge_2 and SiGe clusters, were performed within the density functional theory (DFT) formalism, as implemented in the software tool Hyperchem 8.

We adopted the 6-311G base and the B3LYP for the exchange-correlation functional. The calculations reveal the interatomic distance, heat formation, electron affinity and ionization potential of the studied clusters

4. Results

4.1. Plasma plume Spectra

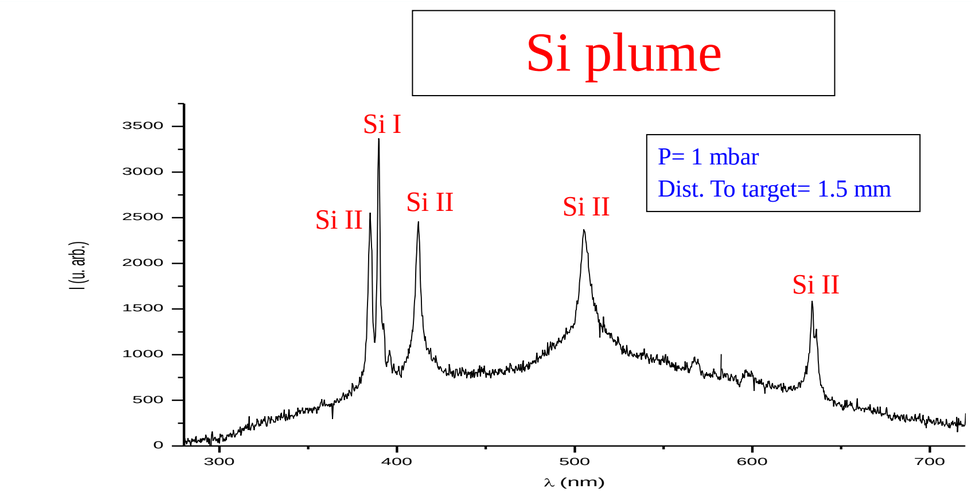

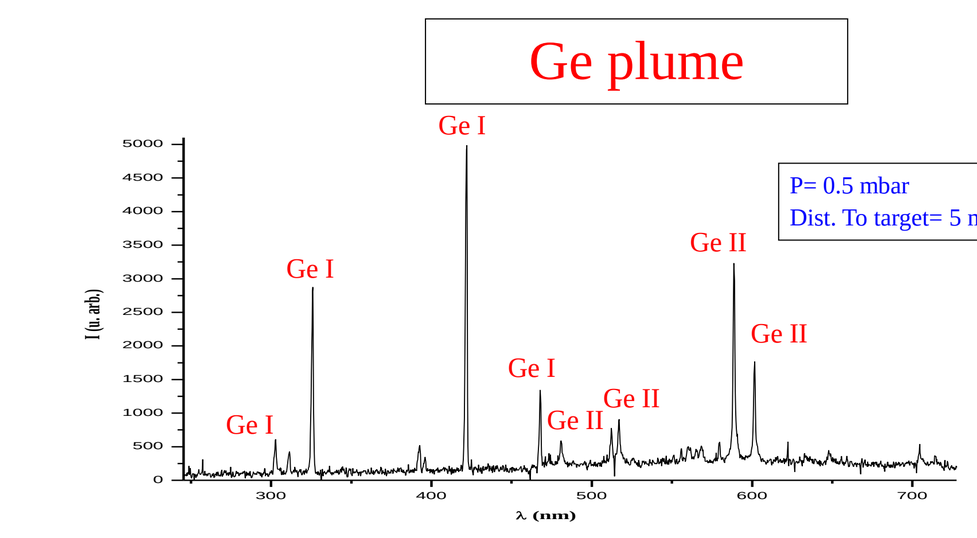

4.2. Ab –initio study of initial particle formation

	r (Å)	Heat of Formation (eV)	Heat of Formation by ions (eV)		r anion (Å)	Electron Affinity (eV)	r cation (Å)	Ionization Potential (eV)
Si_2	2.24	$Si + Si \text{ -----> } Si_2$	$Si^+ + Si^- \text{ -----> } Si_2$		2.17	1.99	2.51	7.89
		-3.71	-9.89					
Ge_2	2.28	$Ge + Ge \text{ -----> } Ge_2$	$Ge^+ + Ge^- \text{ -----> } Ge_2$		2.30	1.91	2.52	7.61
		-2.56	-9.66					
SiGe	2.27	$Si + Ge \text{ -----> } SiGe$	$Si^+ + Ge^- \text{ -----> } SiGe$	$Si^- + Ge^+ \text{ -----> } SiGe$	2.21	1.94	2.52	7.73
		-3.12	-9.88	-9.63				

	Electron Affinity (eV)
Si	1,23
Ge	0,64

Other calculations (6-311G base and B3LYP functional) and experimental data.

	r (Å)	r anion (Å)	Binding Energy (eV)	Binding Energy (eV) experimental	Electron Affinity (eV)	Electron Affinity (eV) experimental
Si_2 [a)]			3.08			
SiGe [a)]	2.22		2.9			
Ge_2 [b)]	2.40	2.31	2.68	2,70±0,07 [c)]	1.93	2,035±0,001
Ge [b)]					1.33	1,232712±0,000015 [d)]

[a)] Edet F. Archibong and Alain St-Aman, J. Chem. Phys.109, 962 (1998)

[b)] Si-Dian Li, Zhi-Guang Zhao, Xiu-Feng Zhao, Hai-Shun Wu, Zhi-Hao Jin, Phys. Rev. B 64, 195312 (2001)

[c)] I.E. Kingcade, H.M. Nagarathna-Naik, I. Shim, K.A. Gingerich, J. Phys. Chem. 90, 2830 (1986).

[d)] M. Scheer, R. C. Bilodeau, C. A.Brodie, H. K. Haugen, Phys. Rev. A 58, 2844 (1998)

4.3. Electronic Temperature. Boltzmann Plot.

The electron temperature was estimated through the Boltzmann plot method. For Si plumes we used SiII specie and for Ge plumes the GeII specie.

$$\ln\left(\frac{I\lambda}{Ag_k}\right) = b - \left(\frac{E_k}{kT_e}\right)$$

I is the intensity of the spectral line, A the transition probability, g_k and E_k are the statistical weight and energy of level k, and kTe the electron temperature in eV.

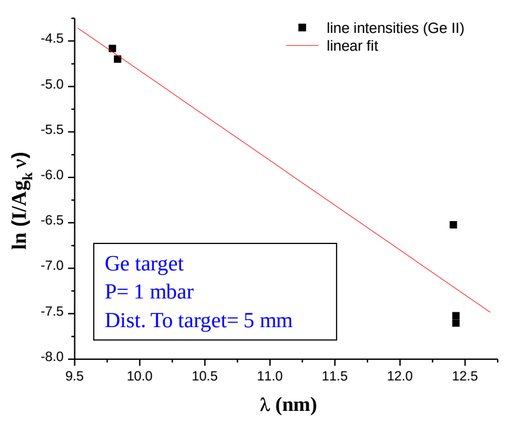

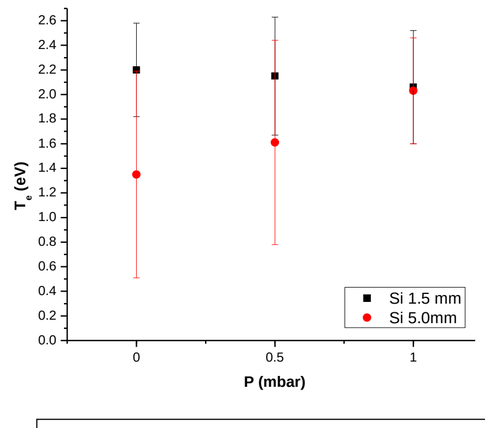

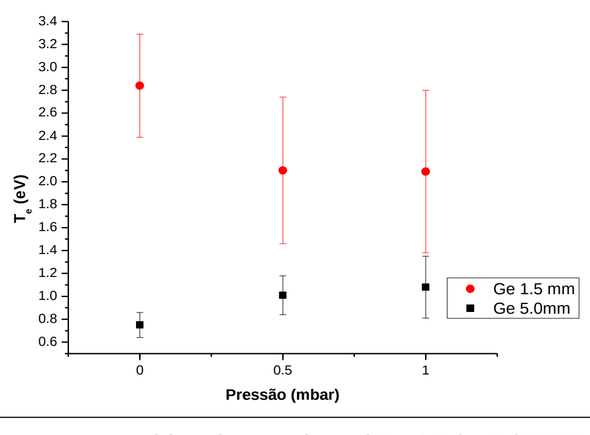

4.4. Electronic density. Stark broadening.

The electron density was estimated through the stark broadening of line SiII (385nmm) for Si plumes and line GeII (602 nm) for Ge plumes.

$$\Delta\lambda_{observed} \approx \Delta\lambda_{instrument} + 2W\left(\frac{Ne}{10^{16}}\right)$$

W is electron impact parameter, and Ne the electron density in cm^{-3}.

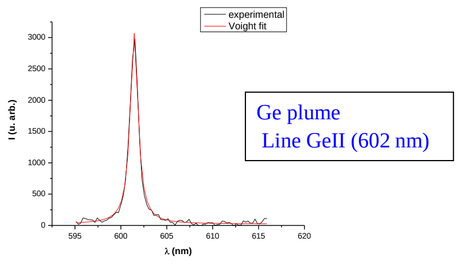

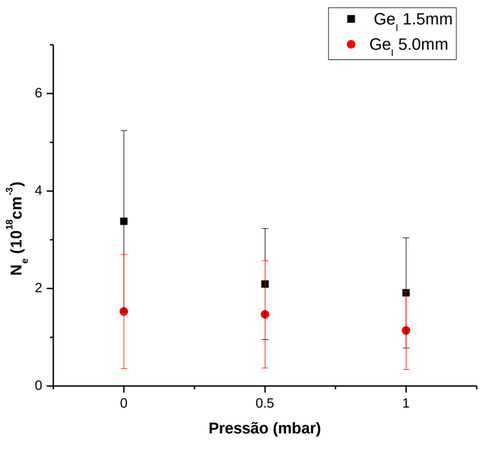

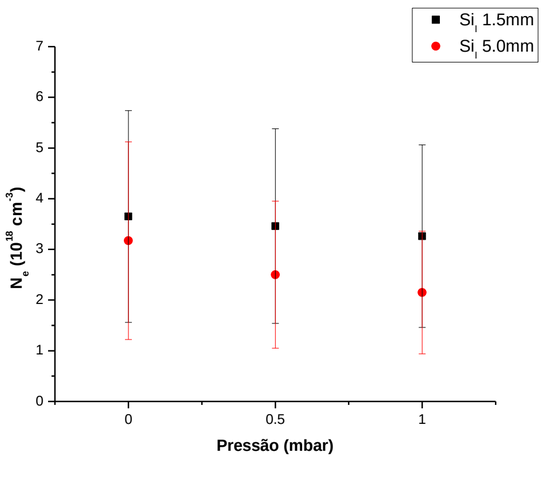

Acknowledgements: This work was supported by the project (PTDC/FIS/098943/2008) funded by the Portuguese Foundation for Science and Technology (FCT).